

# Suppressing Epileptiform Dynamics in Small Hodgkin-Huxley Neuron Clusters via Target Repeller-Attractor Feedback

Sergey Borisenok<sup>1,2</sup>

<sup>1</sup>Department of Electrical and Electronics Engineering, Faculty of Engineering, Abdullah Gül University, Sümer Campus, 38080 Kayseri, Turkey

<sup>2</sup>Feza Gürsey Center for Physics and Mathematics, Boğaziçi University, Kandilli Campus, 34684 Istanbul, Turkey

## Abstract:

**Model:** Small neuron clusters can demonstrate the hypersynchronized epileptiform regime which is very similar to the real human brain epilepsy. The model of Hodgkin-Huxley neuron driven by the stimulating current coming from the axon is used in our approach for a single cell. One of the neurons plays a role of a control element acting autonomously: it tracks the outputs of other companions in the cluster and detects the epileptiform behavior in the collective dynamics. This control element possesses a feedback loop to some part of the cluster neurons and sends the signal to their inputs to suppress the epileptiform regime.

**Methods:** The Kolesnikov's sub-optimal feedback algorithm is used together with our approach of the 'control back propagation' in the network. It consists of two parts: the target repeller (the main part of the algorithm) tends to break the hypersynchronization through all dynamical evolution, while the target attractor based on the control neuron sub-system drives its feedback signal to form and support the dynamical target repeller.

**Results:** We derive analytically all basic equations restoring the necessary control signals in the feedback loop and perform numerical simulations for our proposed model. Our algorithm is robust: it is stable under the perturbation of the initial conditions and the relatively small external noise.

**Key Word:** Hodgkin-Huxley neuron; Epileptiform Dynamics; Kolesnikov's Feedback.

Date of Submission: 14-07-2020

Date of Acceptance: 29-07-2020

## I. Introduction: Network Hierarchy for Epileptiform Mathematical Modeling

Small artificial neuron clusters can demonstrate the hypersynchronized epileptiform regime which is very similar to the real human brain local epilepsy. The mathematical approaches for modeling epileptiform behavior in such networks described in the literature could be systematized according to the network scales<sup>1-3</sup>, as it is presented in the Table 1.

**Table 1.** Hierarchic levels for epileptiform behavior modeling.

	Hierarchic Level	Standard terminology
1	Microscopic (detailed modeling of neural cells)	Detailed network models <sup>4</sup>
2	Low mesoscopic (neural clusters)	Upper level detailed network models, Neural clusters
3	High mesoscopic (neural populations presented with the coupling of NMMs and/or distributed neural fields)	Neural mass models (NMMs), Neural field models <sup>5,6</sup>
4	Macroscopic	Virtual epileptic patient, Epileptor <sup>7</sup>

The classification in Table 1 follows the statistical physics hierarchy for micro-, meso- and macro-scales. In this work we focus on the level of neural clusters.

Neural signal processing plays an increasingly important role in therapeutics, in such applications as neural prosthetics, where electrical signals are read out of the brain and used to control an artificial limb, in closed loop brain stimulation. A series of experiments demonstrate that few factors should be present in the functioning of neural cell clusters: temporally structured input, dependency on prior experience, competition between clusters and control of their activation<sup>8</sup>.

Here we develop our model approach<sup>9</sup>, where the epileptiform regime in a small cluster of mathematical neurons is suppressed by a feedback signal coming from a single control element ('control neuron') acting autonomously. We use the Hodgkin-Huxley ordinary differential equation system to model biological neurons.

The control approach presented here describes a totally novel target repeller algorithm based on Kolesnikov's 'synergetic' approach<sup>10-11</sup>. In our present approach there is no need to divide the control algorithm into two different phases, the detecting of the epileptiform behavior and its further suppression, like it was in our previous model<sup>9</sup>; it deals with both processes simultaneously.

## II. Model for the Small Cluster of Hodgkin-Huxley Neurons

For simplicity let's consider the basic structure of the neural cluster with two working neurons 1 and 2 which can enter to an epileptiform regime of hypersynchronization, and the third control element 3 getting the output signals from 1 and 2 and sending the feedback control over the cluster dynamics to the neuron 2, see Figure 1. Such a network could be a sub-set of a bigger network providing the input currents  $I_{input1}$  and  $I_{input2}$  stimulating the dynamics of the corresponding cells.

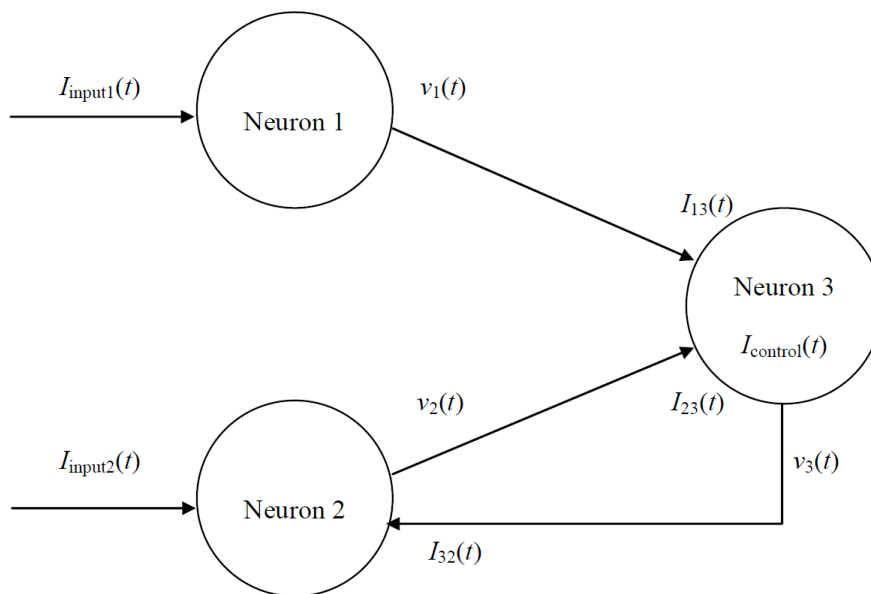


**Figure 1.** Basic model for an epileptiform suppression in the cluster of three Hodgkin-Huxley neurons<sup>9</sup>.

All the currents connecting the neurons follow the same notation type: the current  $I_{kl}$ , is the output for the  $k$ -th neuron and the input for the  $l$ -th neuron. The neurons 2 could be driven by the feedback current  $I_{32}$  coming from the control element. This current will be used for suppressing the hypersynchronized dynamics in the network.

The neuron 3 does not get external currents from other parts of a bigger network. It just collects the currents of the neurons 1 and 2 to detect the possible hypersynchronized regime. Apart from it, the third element has an inner control algorithm  $I_{control}$ , which is shown in Fig. 1 inside the third circle.

It is important to mention that it is not an external current coming from outside, but the inner control free function of the neuron 3. Recently we proposed the similar model<sup>9</sup> for different type of control feedback.

Thus, the current  $I_{control}(t)$  in Fig. 1 corresponds to the autonomous work of the control neuron 3 and must be formulated in the frame of a certain feedback algorithm based only on the input currents  $I_{13}(t)$  and  $I_{23}(t)$ . The explicit formulation of this algorithm in the form of Kolesnikov's feedback is the main goal of our present research.

**Hodkin-Huxley neuron.** The  $k$ -th neuron in the cluster is presented via the Hodgkin-Huxley (HH) nonlinear ordinary differential equation system<sup>4</sup>:

$$\begin{aligned} \frac{dv_k(t)}{dt} &= -\frac{1}{C_M} g\{v_k(t), m_k(t), n_k(t), h_k(t)\} + \frac{I_k(t)}{C_M}; \\ \frac{dm_k(t)}{dt} &= \alpha_m \{v_k(t)\} \cdot [1 - m_k(t)] - \beta_m \{v_k(t)\} \cdot m_k(t); \\ \frac{dn_k(t)}{dt} &= \alpha_n \{v_k(t)\} \cdot [1 - n_k(t)] - \beta_n \{v_k(t)\} \cdot n_k(t); \\ \frac{dh_k(t)}{dt} &= \alpha_h \{v_k(t)\} \cdot [1 - h_k(t)] - \beta_h \{v_k(t)\} \cdot h_k(t). \end{aligned} \quad (1)$$

Here we define the notation for the following ‘conductivity functional’:

$$g\{v_k(t), m_k(t), n_k(t), h_k(t)\} = g_{Na} m_k^3(t) h_k(t) \cdot [v_k(t) - E_{Na}] + g_K n_k^4(t) \cdot [v_k(t) - E_K] + g_{Cl} \cdot [v_k(t) - E_{Cl}]. \quad (2)$$

and the phenomenologically observed membrane gate functionals<sup>4</sup>:

$$\begin{aligned} \alpha_m \{v_k(t)\} &= \frac{0.1 \cdot [25 - v_k(t)]}{\exp\left[\frac{25 - v_k(t)}{10}\right] - 1}; \quad \beta_m \{v_k(t)\} = 4 \cdot \exp\left[-\frac{v_k(t)}{18}\right]; \\ \alpha_n \{v_k(t)\} &= \frac{0.01 \cdot [10 - v_k(t)]}{\exp\left[\frac{10 - v_k(t)}{10}\right] - 1}; \quad \beta_n \{v_k(t)\} = 0.125 \cdot \exp\left[-\frac{v_k(t)}{80}\right]; \\ \alpha_h \{v_k(t)\} &= 0.07 \cdot \exp\left[-\frac{v_k(t)}{20}\right]; \quad \beta_h \{v_k(t)\} = \frac{1}{\exp\left[\frac{30 - v_k(t)}{10}\right] + 1}. \end{aligned} \quad (3)$$

The system (1) contains four dynamical variables: one for the axon action potential  $v_k(t)$  forming the current entering the companion cells, and three membrane gate variables  $\{m_k(t), n_k(t), h_k(t)\}$  which describe the probability for the gates to be open or closed. The summary current  $I_k(t)$  is formed with all external currents entering the  $k$ -th cell. It plays a role of an external signal stimulating the HH neuron dynamics. Particularly:

$$\begin{aligned} I_1(t) &= I_{input1}(t); \\ I_2(t) &= I_{input2}(t) + I_{32}(t); \\ I_3(t) &= I_{13}(t) + I_{23}(t) + I_{control}(t). \end{aligned} \quad (4)$$

The functional (2) includes also the set of constants: the potentials  $E_{Na}$  (equilibrium potential at which the net flow of  $Na$  ions is zero),  $E_K$  (equilibrium potential at which the net flow of  $K$  ions is zero),  $E_{Cl}$  (equilibrium potential at which leakage is zero) in mV, the membrane capacitance  $C_M$  and the conductivities  $g_{Na}$  (sodium channel conductivity),  $g_K$  (potassium channel conductivity),  $g_{Cl}$  (leakage channel conductivity) in mS/cm<sup>2</sup>:

$$\begin{aligned} g_{Na} &= 120; \quad E_{Na} = 115; \\ g_K &= 36; \quad E_K = -12; \\ g_{Cl} &= 0.3; \quad E_{Cl} = 10.36. \end{aligned} \quad (5)$$

Altogether Eqs.(1)-(5) define nonlinear dynamics of HH neuron, which covers the resting, regular spiking and chaotic bursting regimes. We remind here that the spiking/bursting dynamics in the  $k$ -th neuron could be observed only if the input current  $I_k$  overcomes a certain threshold level.

**Action potential transfer.** For the transfer function from the action potential in the axon of the  $k$ -th neuron via its synapses towards the dendrite/soma input of the  $l$ -th neuron we use the simplified gain model<sup>9</sup>:

$$I_l(t) = \alpha \cdot [v_k(t) - v_{rest}]; \quad \alpha = \text{const} > 0, \quad (6)$$

with the constant gain coefficient  $\alpha$  and the phenomenological constant reference rest potential of the HH neuron<sup>4</sup>:

$$v_{rest} = 58 \cdot \log \left( \frac{P_K \cdot K_{ext} + P_{Na} \cdot Na_{ext} + P_{Cl} \cdot Cl_{ext}}{P_K \cdot K_{int} + P_{Na} \cdot Na_{int} + P_{Cl} \cdot Cl_{int}} \right);$$

$$K_{ext} = 20; K_{int} = 400; Na_{ext} = 440; Na_{int} = 50;$$

$$Cl_{ext} = 560; Cl_{int} = 150; P_K = 1; P_{Na} = 3; P_{Cl} = 0.45.$$
(7)

Particularly, following Fig.1,

$$I_{13}(t) = \alpha \cdot [v_1(t) - v_{rest}];$$

$$I_{23}(t) = \alpha \cdot [v_2(t) - v_{rest}];$$

$$I_{32}(t) = \alpha \cdot [v_3(t) - v_{rest}].$$
(8)

In the model (6)-(8) we neglected some effects observed in the real neurons: the time delay in the action potential transfer, the ‘cumulative’ effect of the currents coming from the denrites and stimulating the soma, and some others.

### III. Target Repeller-Attractor Control Algorithm

The system (1) during its nonlinear evolution can enter into a hypersynchronized regime, which has some features of epileptiform dynamics.

Recently we studied Fradkov’s speed gradient control algorithm<sup>12</sup> to provide the suppression of the epileptiform regime. In our previous research<sup>4</sup> the control algorithm in a small HH neural cluster consisted of two parts: the detection of the hypersynchronization and the suppressing feedback, see Figure 2. The feedback control has been switched on only if two potentials,  $v_1$  and  $v_2$ , became hypersynchronized in time.

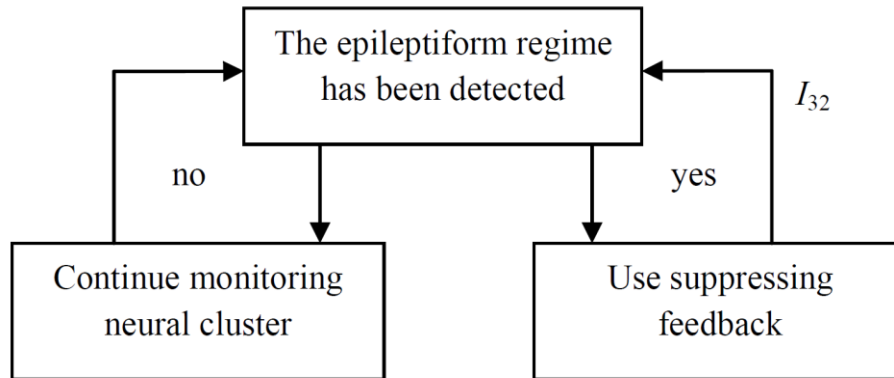


Figure 2. The principle scheme of epileptiform monitoring and speed gradient control algorithm<sup>9</sup>.

It means that the neuron 3 in the algorithm in Fig.2 did not send the feedback signal  $I_{32}$  to the neuron 2 if the epileptiform regime has not been detected, and out of this regime the action potential  $v_3$  was absent.

In our present approach the algorithm forms the repeller acting permanently and driving the system out of hypersynchronization. The second component of the control scheme, the attractor, is responsible for forming and supporting the repeller itself, see the details below.

**Target repeller-attractor system.** Here we follow a different approach, when the target repeller  $R_{12}$  formed in the systems for the neurons 1 and 2 tends to break the hypersynchronization through all dynamical evolution, while the target attractor  $A_3$  based on the sub-system related to the control neuron 3 drives the feedback signal to form the repeller.

Thus, in our present algorithm the feedback loop in Fig.1 works permanently: the target repeller  $R_{12}$  based on the dynamical sub-system of the neurons 1 and 2 suppresses the possible epileptiform behavior, while the target attractor  $A_3$  based on the neuron 3 drives the system (1) out of the hypersynchronization regime via correcting the structure of the dynamical repeller  $R_{12}$  using the feedback loop, see Figure 3.

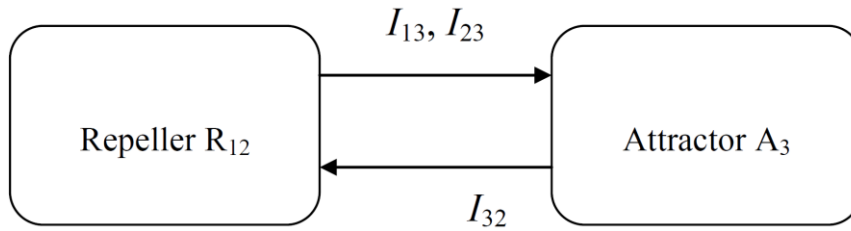


**Figure 3.** Target repeller-attractor algorithm used in the present paper.

The repeller  $R_{12}$  in our system is dynamical: it depends on the input currents  $I_{input1}(t)$  and  $I_{input2}(t)$ . To construct it, let's re-formulate here Kolesnikov's approach for a target repeller. Usually this approach has been used to form in the dynamical system a target attractor locking the phase trajectories in its neighborhood<sup>10-11</sup>.

In this paper we re-formulate the method to form the target repeller in the system to break the hypersynchronization. Kolesnikov's sub-optimal feedback algorithm is used together with our 'control back propagation' scheme<sup>9,13</sup>.

**Construction of the repeller.** The repeller  $R_{12}$  in our dynamical system must act on the subsystem related to the neurons 1 and 2. Following basic Kolesnikov's approach<sup>11</sup>, let's define the target function:

$$\psi_{12}(t) = v_2(t) - v_1(t) , \tag{9}$$

measuring the rate of (hyper)synchronization between the neurons 1 and 2. Our goal is to drive the system exponentially far away from small  $\psi_{12}$ , such that we can define the control as:

$$\frac{d\psi_{12}(t)}{dt} = \frac{1}{T_{12}} \cdot \psi_{12}(t) , \tag{10}$$

with the positive constant  $T_{12}$ . The positive sign in RHS(10) correspond to the repeller with the exponentially divergent trajectories. Using (10), (4) and first equation of the system (1) for the neurons 1 and 2, we get:

$$I_{32}^{(*)}(t) = \frac{C_M}{T_{12}} \cdot [v_2(t) - v_1(t)] + g\{v_2(t), m_2(t), n_2(t), h_2(t)\} - g\{v_1(t), m_1(t), n_1(t), h_1(t)\} + I_{input1}(t) - I_{input2}(t) . \tag{11}$$

The upper index (\*) for the current  $I_{32}$  shows that (10) is a target function to form the repeller (9)-(10). It must be designed as a result of our control in the neuron 3 with the output action potential  $v_3$ , see Fig.1. (the 'control back propagation' scheme<sup>9,13</sup>). By the transfer model (6) it implies:

$$v_3^{(*)}(t) = v_{rest} + \frac{I_{32}^{(*)}(t)}{\alpha} . \tag{12}$$

Thus, the target potential for the control neuron 3 is given by (12). It is the time-dependent function, so, the control goal here is a tracking.

**Construction of the attractor.** The attractor  $A_3$  in our dynamical system is related to the sub-system of the neuron 3. The goal of this attractor is to form the output signal (12) by the control current  $I_{control}$ . To restore the necessary control current, let's again take Kolesnikov's algorithm<sup>11</sup> in the form

$$\psi_3(t) = v_3(t) - v_3^{(*)}(t) , \tag{13}$$

and

$$\frac{d\psi_3(t)}{dt} = -\frac{1}{T_3} \cdot \psi_3(t) , \tag{14}$$

with the positive constant  $T_3$ . The negative sign in RHS(14) stands for the forming attractor, tracking the target potential (12).

By (13)-(14) and by the first equation of the system (1) for the third neuron, we get for the target  $I_3$ :

$$I_3^{(*)}(t) = C_M \frac{dv_3^{(*)}(t)}{dt} - \frac{C_M}{T_3} \cdot [v_3(t) - v_3^{(*)}(t)] + g\{v_3(t), m_3(t), n_3(t), h_3(t)\} . \tag{15}$$

Finally, using (4) for the currents entering the third neuron, and (6) for the outputs  $v_1$  and  $v_2$ , we get:

$$I_{\text{control}}(t) = I_3^{(e)}(t) - \alpha \cdot [v_1(t) - v_{\text{rest}}] - \alpha \cdot [v_2(t) - v_{\text{rest}}]. \quad (16)$$

The set of Eqs.(11), (12), (15) and (16) forms the feedback algorithm.

Thus, we've constructed a target pair 'repeller-attractor' in our dynamical system.

#### IV. Numerical Simulations

For the purpose of numerical simulations the following set of parameters has been chosen:

$$I_{\text{input1}} = 50 ; I_{\text{input2}} = 52 ; C_M = 1 ; \alpha = 0.5 ; T_{12} = 0.1 ; T_3 = 0.02 . \quad (17)$$

The motivation for the numerical set (17) is following. The gain coefficient  $\alpha$  should be in accordance with experimental data. The input currents  $I_{\text{input1}}$  and  $I_{\text{input2}}$  must be greater than a threshold level; and they are chosen to be closed each to other to cause the epileptiform regime in the network.

The constants  $T_{12}$  and  $T_3$  define the typical time scales for the re-forming the repeller  $R_{12}$  (9)-(10) and the attractor  $A_3$  (13)-(14) due to the change of the input currents and the inner evolution of the dynamical system (1). According to the proposed algorithm, the attractor  $A_3$  is responsible for fitting the repeller  $R_{12}$  to the changing dynamics, thus, it should work faster. That implies the inequality for the time constants:  $T_3 \ll T_{12}$ .

The results of the simulations are presented in Figure 4.

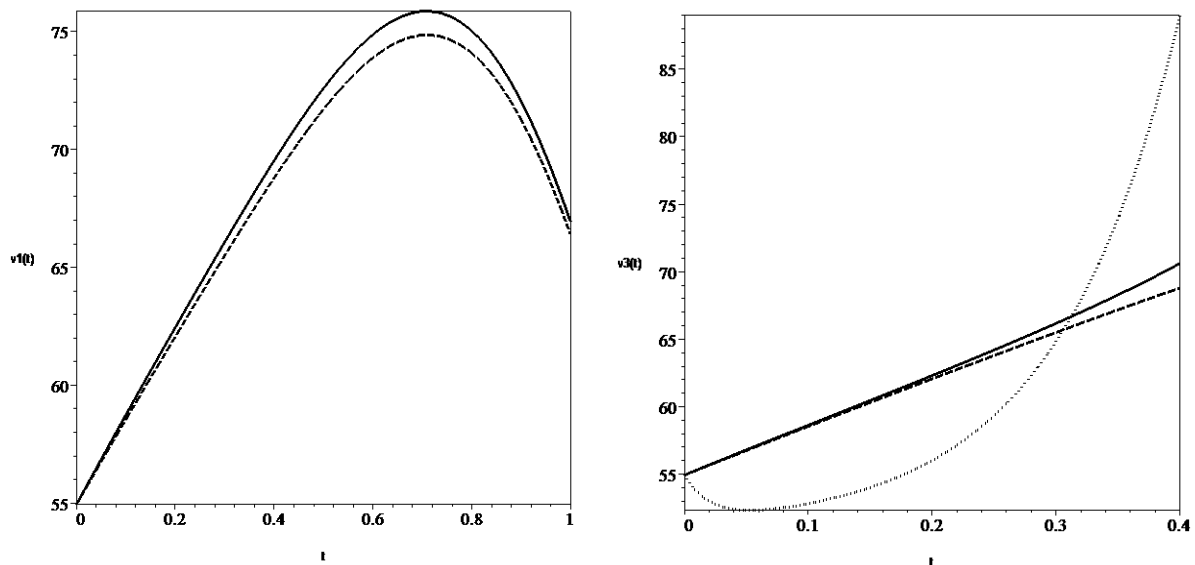


**Figure 4.** Numerical simulations for suppressing of the epileptiform regime in the dynamics of the neurons 1 and 2 via the feedback of the control neuron 3. The action potentials for  $v_1$  (dash line),  $v_2$  (solid line) and control  $v_3$  (dot line) are plotted vs time  $t$ . **Left:** No feedback loop in Fig.1 ( $I_{32} = 0$  and  $v_3 = 0$ ); **Right:** There is a target repeller-attractor feedback loop.

In Figure 4 we plot the action potentials for all three neurons from our cluster. The potential of the neuron 3 is actually a control signal entering the neuron 2, see (12). We present here the potential  $v_3$ , not the current  $I_{32}$ , just to keep the same units for all three functions. One can see that the numerical results demonstrate the efficiency of the control algorithm. Without Kolesnikov's control in Fig.4 (left) one can observe the epileptiform regime of two hypersynchronized neurons 1 and 2. In the presence of our control algorithm in Fig.4 (right) the repeller drives the second neuron far away from the epileptiform dynamics. The result of numerical simulations does not depend sufficiently on the initial conditions of the system (1).

There is no need to measure the rate of hypersynchronization as it was done in the previous algorithm<sup>9</sup>. The dynamical repeller provides the exponential divergence of the trajectories at the typical time scale  $T_{12} = 0.1$  for all neighborhoods of (9).

#### V. Conclusion and Further Considerations

The algorithm proposed in the paper is universal and does not depend on the initial conditions of the dynamical variables. Our algorithm is robust: it is stable under the perturbation of the initial conditions and the

relatively small external noise. It can be easily extended for a bigger number of neurons participating in the epileptiform dynamics.

The construction of the repeller in the dynamical system is natural in the frame of Kolesnikov's algorithm. Nevertheless, the construction of the dynamical attractor via the feedback loop of the neuron 3 could be performed in the frame of any optimal or suboptimal approaches: Pontryagin's optimal control, Fradkov's speed gradient<sup>12</sup>, and others. Pros and cons of different approaches will be a matter of our following research.

### References

- [1]. Mehta MR, Dasgupta C, Ullal GR. A neural network model for kindling of focal epilepsy: Basic mechanism. *Biological Cybernetics*, 1993; 68(4): 335-340.
- [2]. Wulsin DF, Fox EB, Litt B. Modeling the complex dynamics and changing correlations of epileptic events. *Artificial Intelligence*, 2014; 216: 55-75.
- [3]. Jedynak M, Pons AJ, Garcia-Ojalvo J. Collective excitability in a mesoscopic neuronal model of epileptic activity. *Physical Review E*, 2018; 97: 012204.
- [4]. Hodgkin AL, Huxley AA. A quantitative description of membrane current and its application to conduction and excitation in nerve. *Journal of Physiology*, 1952; 117: 500-544.
- [5]. Zetterner LH, Kristiansson L, Mossberg K. Performance of a model for a local neural population. *Biological Cybernetics*, 1978; 31: 15-26.
- [6]. Cosandier-Rimele D, Badier JM, Chauvel P, Wendling F. Modeling and interpretation of scalp-EEG and depth-EEG signals during interictal activity. *Conference Proceedings: IEEE Engineering in Medicine and Biology Society 2017*, 4270-4280.
- [7]. Jirsa VK, Proix T, Perdikis D, Woodman MM, Wang H, Gonzalez-Martinez J, Bernard C, Benar C, Guye M, Chauvel P, Bartolomei F. The virtual epileptic patient: Individualized whole-brain models of epilepsy spread. *Neuroimage*, 2017; 145: 377-388.
- [8]. Mitra, PP, Bokil H. *Observed Brain Dynamics*. Oxford, New York: Oxford University Press, 2008.
- [9]. Borisenok S, Çatmabacak Ö, Ünal Z. Control of collective bursting in small Hodgkin-Huxley neuron clusters. *Communications Faculty of Sciences University of Ankara Series A2-A3*, 2018; 60: 21-30.
- [10]. Kolesnikov A. *Synergetic Control Methods for Complex Systems*. Moscow: URSS Publ, 2012.
- [11]. Kolesnikov A. Introduction of synergetic control, 2014 American Control Conference, Portland, 3013-3016.
- [12]. Fradkov AL. *Cybernetical Physics: From Control of Chaos to Quantum Control*. Berlin, Heidelberg: Springer, 2017.
- [13]. Borisenok S, Ünal Z. Tracking of arbitrary regimes for spiking and bursting in the Hodgkin-Huxley neuron. *MATTER: International Journal of Science and Technology*, 2017; 3: 560-576.

Sergey Borisenok. "Suppressing Epileptiform Dynamics in Small Hodgkin-Huxley Neuron Clusters via Target Repeller-Attractor Feedback." *IOSR Journal of Mathematics (IOSR-JM)*, 16(4), (2020): pp. 41-47.